

Fine-scale density wave structure of Saturn's A, B, and C rings

Evgeny Griv

Department of Physics, Ben-Gurion University of the Negev, Beer-Sheva 84105, Israel
email: griv@bgumail.bgu.ac.il

Abstract. In view of the possibility of employing *Cassini's* experiments for the diagnosis of the Saturnian ring system, local N -body simulations of low and moderately high optical depth regions of Saturn's main rings are presented. A special emphasis is made on fine-scale spiral structures (irregular cylindrical wave-type structures of the order of 100 m or so) of Saturn's A, B, and C rings. It is predicted that *Cassini* spacecraft high-resolution images of Saturn's rings will reveal this kind of small-scale irregular density wave structure.

Keywords. Planets, Saturn's rings, waves and instabilities, N -body simulations

1. Introduction

Voyager images of Saturn's main A, B, and C rings have shown evidence of radial structures ranging from a few kilometres down to the several hundreds metres resolution of the spacecraft's camera (Smith *et al.* 1982). The best resolution demonstrated structures at all scales in the rings, down to the limit of resolution ~ 5 km. Most of the structures are irregularly spaced and do not correspond to resonances with known satellites. It is important that the *Voyager's* stellar occultation data revealed some indirect evidence for structuring in the densest central parts of Saturn's B ring down to 100 m length scale. One cannot exclude the existence of a fine irregular structure of this kind in other regions of the Saturnian ring system of mutually gravitating and colliding particles.

Among all mechanisms, the self-excited nonresonant Jeans instability of gravity disturbances (e.g., those produced by a spontaneous perturbation or a satellite system) has long been suspected to be the key one that determines the ubiquitous irregular structure of Saturn's rings, with the appearance of record-grooves (e.g., Esposito 1993, Fig. 5 therein; Cuzzi *et al.* 2002, Fig. 2b therein). Accordingly, a system of mutually gravitating particles of Saturn's rings exhibits collective, gravitationally unstable modes of motions. A quasi-linear kinetic theory of the almost aperiodic Jeans instability in Saturn's rings has been developed by Griv *et al.* (2000, 2003a, 2003b) and Griv & Gedalin (2003). The theory predicts that as a direct result of the instability of small-amplitude gravity disturbances the main parts of A, B, and C rings are divided into numerous irregular spiral ringlets of the order of 2π times the local thickness $h = 5 - 30$ m. Below I describe N -body simulations in order to verify the validities of the theory.

2. Local simulations

The dynamical behavior of planetary rings has already studied via simplified N -body simulations of an orbiting patch of the ring by Salo (1992, 1995), Richardson (1994), Osterbart & Willerding (1995), Sterzik *et al.* (1995), Griv (1998), Daisaka & Ida (1999), and others. See Griv & Gedalin (2003) as a review of the problem. In these N -body experiments in a local, or Hill's approximation dynamics of particles in small regions

of the disk are assumed to be statistically independent of dynamics of the particles in other regions. The local numerical model thus simulates only a small part of the system and more distant parts are represented as copies of the simulated region. The system of Newton's equations of three-dimensional motion in local approximation for $N \gg 1$ identical particles,

$$\frac{d^2x}{dt^2} - 2\Omega r_0 \frac{d\Omega}{dr} x - 2\Omega \frac{dy}{dt} = F_x, \quad (2.1)$$

$$\frac{d^2y}{dt^2} + 2\Omega \frac{dx}{dt} = F_y, \quad (2.2)$$

$$\frac{d^2z}{dt^2} + \Omega^2 z = F_z, \quad (2.3)$$

was integrated by the Runge–Kutta method of the fourth order. In Eqs. (2.1)–(2.3),

$$x = r - r_0, \quad y = r_0(\varphi - \Omega t),$$

r_0 is the reference radius, $\Omega = \Omega(r_0)$, and $A_0 = -(r_0/2)(d\Omega/dr)_0 \approx (3/4)\Omega$ is the first Oort constant of the differential rotation which is a measure of the shear strength. In general, F_x , F_y , and F_z are the forces due to interactions with other particles. The gravitational forces are

$$\vec{F}_i = -G \sum_{j \neq i}^N \frac{(\vec{r}_i - \vec{r}_j)}{[(\vec{r}_i - \vec{r}_j)^2]^{3/2}}, \quad (2.4)$$

where \vec{r}_i is the position of the i -th particle and \vec{r}_j is the position of the j -th particle. Following Wisdom & Tremaine (1988), Salo (1995), Richardson (1995), Daisaka & Ida (1999), and Ohtsuki & Emori (2000), I adopted the standard hard-sphere collision model. A collision changes only impact velocity in normal direction, $v'_n = -\epsilon v_n$ and $v'_t = v_t$, where v_n , v_t and v'_n , v'_t , respectively, are relative velocities of colliding particles in the normal direction and the tangential direction.

A rotating Cartesian coordinate system with origin at the reference position r_0 was chosen, the x axis pointing radially outward and the y axis pointing in the direction of the rotation (Wisdom & Tremaine 1988; Salo 1995; Sterzik *et al.* 1995). The particles were initially placed on nearly circular orbits with an anisotropic Maxwellian (Schwarzschild) distribution of small random velocities. The initial distribution of particles was generated by means of pseudo-random number generator placing particles uniformly in the box in real space. The box should be thought of as being embedded in Saturn's ring disk which has a constant angular velocity gradient in the x direction.

I present simulations which are distinguished primarily by their values of the radial c_r and azimuthal c_φ velocity dispersions. The “cool” model has a value of $c_r \equiv 2c_\varphi = 0.5c_T$, and so I expect the model to be initially violently unstable to both radial and spiral gravity disturbances. Here, $c_T = 3.4G\Sigma_0/\Omega$ is the well-known Safronov–Toomre (Safronov 1960; Toomre 1964) random velocity dispersion to suppress the instability of axisymmetric (radial) disturbances and Σ_0 is the mean (local) surface density of the disk. The “warm” model has $c_r \equiv 2c_\varphi = c_T$, and so it is expected to be unstable only to spiral disturbances. In turn, the “hot” model with $c_r \equiv 2c_\varphi = 2c_T$ is expected to be at best only marginally unstable to the growth of spiral waves. See Griv *et al.* (2000, 2003a, 2003b) and Griv & Gedalin (2003) for an explanation. In all experiments, initially $c_z = 0.2c_r$.

To maintain the system under the shearing stress in a steady state, the cyclic boundary conditions were used in the form suggested by Wisdom & Tremaine (1988), Toomre (1990), Salo (1995), and others. The direction of the disk rotation was taken to be

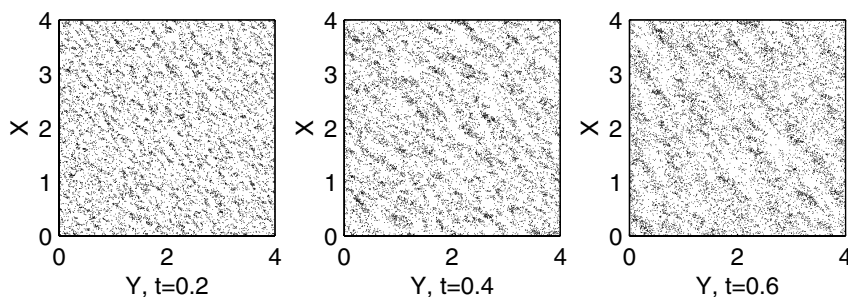


Figure 1. Time-development of the differentially rotating three-dimensional model of particles (face-on view) distributed over the $L_x \times L_y \times L_z = 4\lambda_J \times 4\lambda_J \times \lambda_J$ unit cell; $c_r = 0.5c_T$. The model is violently unstable against spontaneous trailing gravity perturbations.

clockwise. Time $t = 1$ corresponds to a single revolution of the disk, and the orbital period was $T_{orb} = 2\pi/\Omega$. All the particles moved with the same fixed time step $\Delta T = 0.001T_{orb}$. In Saturn's rings, a measure of the fundamental vibration period, or the dynamical time is of the order of $T_{dyn} \sim (G\rho_{ring})^{-1/2} \sim 1$ h if we assume the volume density $\rho_{ring} \sim 1$ g/cm³. This means that $T_{orb} \sim 10T_{dyn}$, so a choice of the stepsize $\Delta T = 0.001T_{orb}$ gives about 100 steps per particle dynamical time, which should be sufficient to accurately resolve particle–particle interactions.

In experiments reported below the following physical parameters for a simulated patch of the ring were chosen: the orbital period $T_{orb} \equiv 2\pi/\Omega = 7.027$ h which corresponds to a typical orbital period of the C ring's particle at the distance $r = 85\,000$ km from the planet, the surface density $\Sigma_0 = 15$ g/cm², and the total number of particles $N = 12\,000$ in all models. The particle radius $r_p = 4.2$ cm in $L_x \times L_y \times L_z = 4\lambda_J \times 4\lambda_J \times \lambda_J$ three-dimensional models. The corresponding Jeans–Toomre wavelength $\lambda_J \approx 6.4$ m and the optical depth $\tau \approx \pi r_p^2 n \approx 0.1$ in all models (n is the number density per unit area). The constant coefficient of restitution was $\epsilon = 0.8$. A very popular model of the particles in Saturn's rings is a smooth ice sphere, whose restitution coefficient is quite high, exceeding 0.63, and decreases as the collision velocity increases (Goldreich & Tremaine 1982; Bridges *et al.* 1984; Kerr 1985). Saturnian ring system is populated primarily by centimeter- to a few meter-sized mutually gravitating and physically colliding particles (Zebker *et al.* 1985). A particle size distribution function exhibits approximately inverse-cubic power-law behavior. In addition, Saturn has extensive but much more tenuous rings containing mainly micrometer-sized particles (Lissauer & Cuzzi 1985). Because low-velocity collisions of ice particles will always involve some dissipation of acoustic energy, some source of energy must be available to keep them from total collapse to a featureless monolayer.

3. Fine-scale structure

In Fig. 1 I show a series of snapshots from a run with the cool model, i.e., the nonuniformly rotating model, in which initially particles all move along almost circular orbits and the radial dispersion of the random velocities is smaller than the critical Safronov–Toomre one, namely $c_r = 0.5c_T$, or Toomre's Q -value, $Q = c_r/c_T$ is equal to 0.5, respectively. As has been predicted in the theory, the Jeans instability develops quickly in the system. Figure 1 clearly shows that in a disk with the Keplerian shear profile a spiral pattern (more accurately, a chainlike structure or irregular “wakes”) develops spontaneously in the initially featureless disk on a dynamical time scale $< \Omega^{-1}$. The wakes are created if self-gravity is included; only collisions do not create the structure.

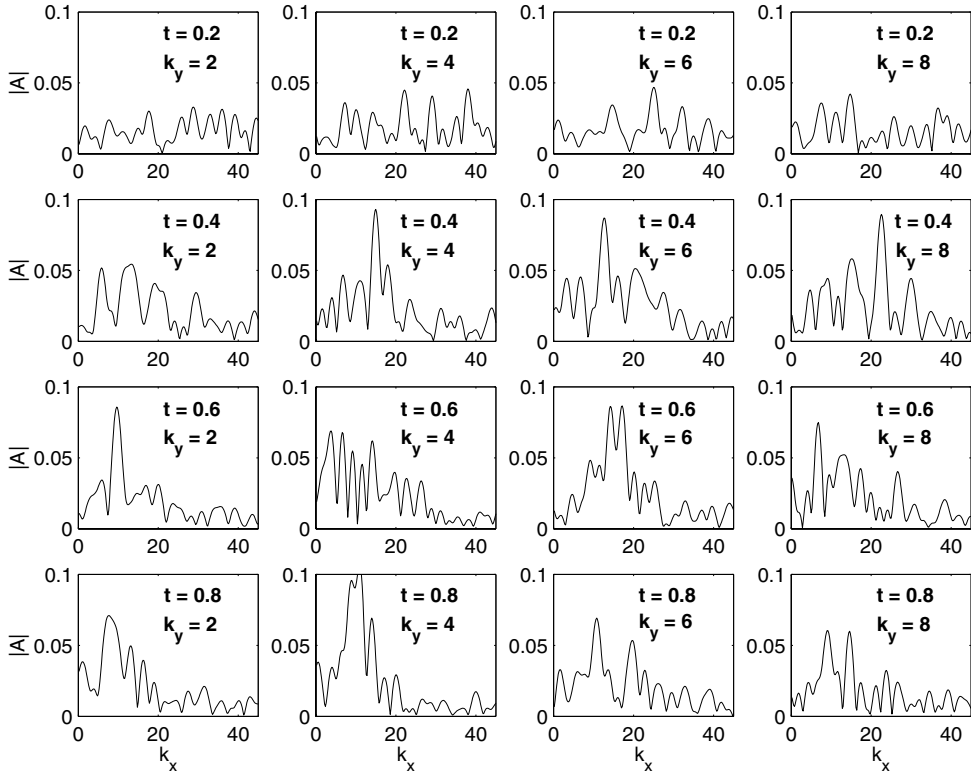


Figure 2. Density spectrum $|A(k_x, k_y)|$ of the particle distribution shown in Fig. 1 for different azimuthal k_y and radial k_x mode numbers at the calculation times $t = 0.2 - 0.8$.

Their pattern speed Ω_p is zero, because the system is spatially homogeneous (Griv *et al.* 2003b). The Lin–Shu type density wave structure (Lin & Shu 1966; Lin *et al.* 1969; Shu 1970; Lin & Lau 1979; Griv & Gedalin 2003) is time dependent and transient.

Early in the evolution, multiple spirals interfere with each other and produce a complicated set of density concentrations. At most, eight or nine individual high-density wakes can be seen (Fig. 1, $t = 0.4 - 0.6$). The structure consists of elongated trailing filaments with a definite pitch angle ψ_{crit} with respect to the local shear flow. The pitch angle of spiral wakes $\psi_{\text{crit}} \approx 20^\circ$ can be obtained by examining Fig. 1 directly.

Figure 1 gives a feeling for the evolutionary process, but in order to trace and quantify the growth of instabilities in the disk, it is necessary to compute Fourier decompositions of the surface density distribution for various mode numbers. Shown in Fig. 2 are the sequences of density-spectrum evolution in the wavenumber space for the case shown in Fig. 1 at the calculation times $t = 0.2 - 0.8$. The power spectrum is constructed by employing a technique where one regards the particle, labeled by j , as a discrete δ -function to calculate the density Fourier component, i.e.,

$$A(k_x, k_y) = \frac{1}{N} \sum_{j=1}^N \exp(\vec{k} \cdot \vec{r}_j). \quad (3.1)$$

In addition, the azimuthal wavenumber k_y assumes discrete values compatible with the finite boundaries in the streamwise direction, that is, in the y -direction, whereas the radial wavenumber k_x assumes continuous values because of the background flow shear. The

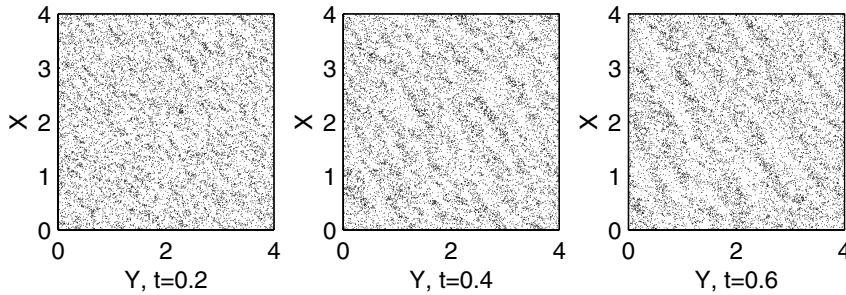


Figure 3. Time-development of the differentially rotating model; $c_r = c_T$. In agreement with the theory, even though the initial radial velocity dispersion c_r is equal to the Safronov–Toomre one c_T , the model is still unstable against nonaxisymmetric perturbations.

pitch angle of a spiral ψ is given by $\psi = \arctan(k_y/k_x)$, and positive k_x corresponds to trailing spirals and negative k_x to leading. The wavenumber is normalized to π/L_y . Thus, the quantity k_y gives the number of halfwaves of a spiral mode of collective oscillations in the y -direction.

No particular set of k_x, k_y dominates at the beginning of calculations ($t = 0.2$), which corresponds to the initial noise. It is evident from Fig. 2 that the $c_r < c_T$ case produces rigorous instabilities. One can clearly see that at times $t \gtrsim 0.6$ a dominant k_y is equal about to $(2L_y/\lambda_J) \tan \psi \approx 4$, which is consistent with the linear stability analysis for the marginally unstable mode (Griv *et al.* 2003b; Griv & Gedalin 2003). That is, a wavelength of the dominant mode in the streamwise direction $\lambda_y = \lambda_{\text{crit}}/\tan \psi \approx 2\lambda_J$, where $\psi = 20^\circ - 25^\circ$. The latter fact convincingly indicates that we have dealt with a collective-type instability rather than with a random process (as advocated by Toomre 1990 and Toomre & Kalnajs 1991). It is natural to attribute the observed instability to the Jeans instability so far discussed in the paper. Also, we see that there are a number of $k_y = 2, k_y = 6$, and $k_y = 8$ discrete harmonics present.

In the second set of experiments with the Keplerian disk, I simulated a system which is stable according to Safronov (1960) and Toomre (1964): the initial radial velocity dispersion is equal to $c_r = c_T$, or Toomre’s parameter $Q = 1$, respectively. The evolution of the model is shown in Fig. 3. As is seen, in a Safronov–Toomre stable disk with the differential rotation a spiral instability develops rapidly on a dynamical time scale $\lesssim \Omega^{-1}$. This fierce instability of the system with $c_r = c_T$ indicates that in a *differentially* rotating system the Jeans instability of *nonaxisymmetric* ($\psi \neq 0$) gravity perturbations cannot be suppressed by the ordinary Safronov–Toomre critical velocity spread $c_T \approx 3.4G\Sigma_0/\Omega$, in line with theoretical expectations (Griv 1996, 1998; Griv & Gedalin 2003).

The initial unstable growth is clear from Figs. 1–3. The simulated wake structure rapidly at times $t \gtrsim 0.6$ reaches nonlinearity, and is thus beyond the scope of our theory (or any corresponding linear analysis of shearing modes). I then simulated a differentially rotating disk which is stable in accordance with the modified stability criterion (Griv *et al.* 2000, 2003a, 2003b; Griv & Gedalin 2003). Figure 4 shows the observed evolution of the dynamically hot model with $c_r = 2c_T$ (or $Q = 2$, respectively). As one can see, in such a system this relatively high “temperature” c_r almost eliminates completely the growth rate of the gravitational instability. In sharp contrast to the previous simulations, the model is now almost gravitationally stable. The contrast between Figs. 1–3 and Fig. 4 establishes experimental evidence to support the stability theory developed by Griv and co-workers. Note that Salo (1995), Richardson (1994), Osterbart & Willerding (1995), Sterzik *et al.* (1995), and Daisaka & Ida (1999) have already found that the stability

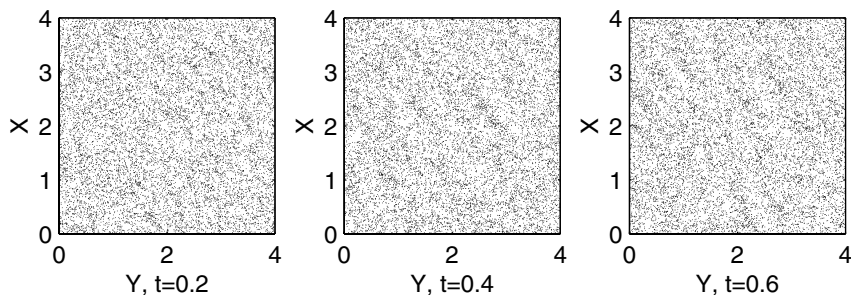


Figure 4. Time-development of the differentially rotating model; $c_r = 2c_T$. All perturbations are almost suppressed, including the most unstable nonaxisymmetric ($\psi \neq 0$) ones.

number Q of Toomre in relaxed equilibrium disks does not fall below a critical value, which lies about $Q_{\text{crit}} = 2 - 2.5$. However, no adequate explanation of the latter has been presented. See also Griv *et al.* (1999) for a discussion of the problem.

4. Vertical structures

Figures 1–3 show the density distributions of unstable models of Saturn’s rings in the plane (face-on view). As has been mentioned by Salo (1992, 1995) and others, another feature of the simulations is the radical changes in vertical structures of unstable systems that result from the instabilities. Figure 5 shows distributions of particles and isodensity contours in the (z, η) -plane for the three-dimensional model at the simulation times $t = 0$ and $t = 0.4$. (I introduced a new coordinate system (z, η) ; η is perpendicular to the spiral wakes, while z gives the normal to the plane position.) The disk surface generally evolves from a smooth height profile with η to complex structures with peaks and valleys that result from instabilities. The results presented in Fig. 5 are consistent with the hypothesis that we have dealt with the even Jeans perturbations, because the perturbed density is an even function of z . This type of vertical motions does not deform the horizontal disk plane $z = 0$, because the vertical velocity v_z in a density wave is odd in z : $v_z(-z) = -v_z(z)$. Such “sausage-like” perturbations (Bertin & Casertano 1982) can release gravitational energy and are subject to classical gravitational Jeans-type instability.

5. Summary

The most puzzling features of Saturn’s rings, revealed by *Voyager* fly-bys, are the radial density variations seen on all scales down to the resolution limit of few kilometers. At the present time, their origin is far from being understood (Tremaine 2003). This paper reports on an investigation of the significance of self-excited (that is, intrinsic), off-resonant, almost aperiodic Jeans instability in Saturn’s main rings to the formation of the fine-scale structures. I explored the linear regime of Jeans instabilities in Saturn’s rings by means of sliding N -body patch model (e.g., Salo 1992, 1995) and compared those numerical results with the quasi-linear kinetic stability theory by Griv *et al.* (2000, 2003a, 2003b) and Griv & Gedalin (2003). The aim of the work is to discuss specific astronomical implications of the study to Saturn’s rings in view of the possibility of employing *Cassini*’s experiments. Summarizing, I claim that

1. In order to suppress the instability of arbitrary but not only axisymmetric Jeans-type perturbations in a differentially rotating disk, including the most unstable nonaxisymmetric ones, the value of the radial dispersion of random velocities of particles must

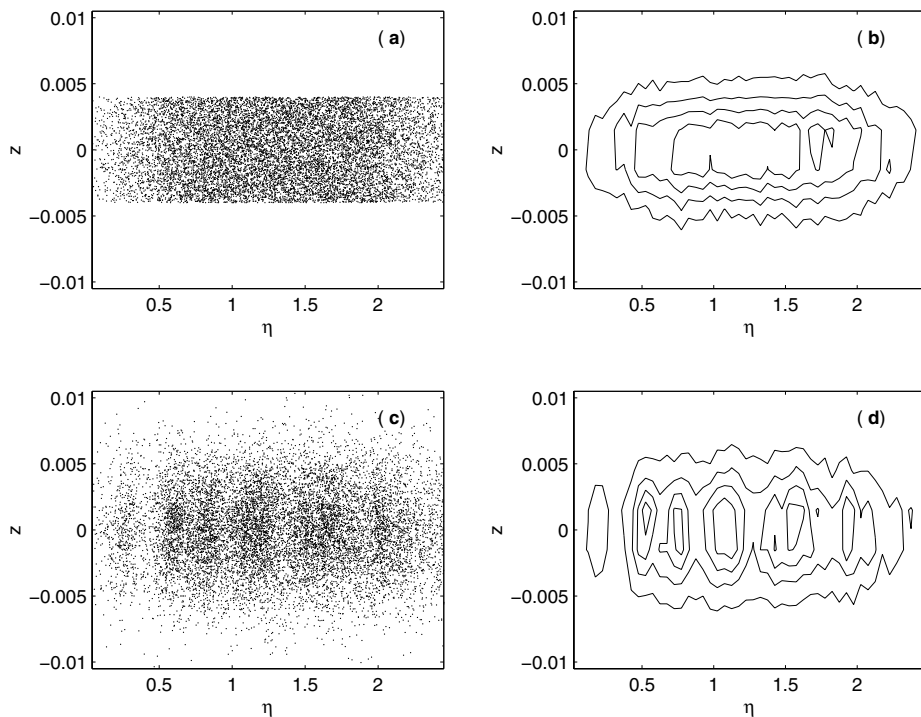


Figure 5. Comparison of vertical structure. Shown are both distributions of particles and isodensity contours in the (z, η) -plane for the three-dimensional model shown in Fig. 3 at the calculation times $t = 0$ and $t = 0.4$: (a) distribution of particles at $t = 0$, (b) isodensity contours at $t = 0$, (c) distribution of particles at $t = 0.4$, and (d) isodensity contours at $t = 0.4$. Figures 5c and 5d give the end-on edge-on views of the positions and isocontours of the density of the disk particles at $t = 0.4$, respectively. The unstable spiral disturbances significantly alter the disk's vertical surface.

exceed $c_{\text{crit}} \approx 2c_T$, or Toomre's stability parameter $Q \gtrsim 2$. It is expected that in the main rings of Saturn $Q \approx 2$ (cf. Lane *et al.* 1982, p. 543). I again argue that sufficient velocity dispersion ($Q \gtrsim 2$) prevents the Jeans instability from occurring but inelastic particle collisions reduce the relative particle velocities so that the Jeans instability may be an effective generating mechanism for the recurrent fine structure of the ring system.

2. In Saturn's rings, this almost aperiodic gravitational instability manifests itself as trailing cylindrical density-wave enhancements, forming $\approx 20^\circ$ angle with respect to tangential direction.

3. By local simulations of a particle model, we see that at the limit of stability with respect to all gravity perturbations of a differentially rotating disk the critical radial wavelength becomes approximately equal to $\lambda_{\text{crit}} = 2\lambda_J$. Modern observations indicate that the ring thickness ranges from 1 – 2 m in the C ring to 1 – 5 m in the B ring and 5 – 30 m in the A ring (Esposito 2002). Then, in the C ring estimations give the value of $\lambda_{\text{crit}} = 6 - 20$ m, in the B ring $\lambda_{\text{crit}} = 6 - 50$ m, and in the A ring $\lambda_{\text{crit}} = 30 - 300$ m. Thus, both the theory and the simulations forecast the existence of the fine-scale ~ 100 m or even less radial structures in Saturn's main rings.

4. Seen edge-on with the fine spirals seen end-on (with the line of sight along the spiral local major axis), Saturn's rings will show even with respect to the equatorial plane "sausage" structures.

Acknowledgements

The author would like to thank Tzi-Hong Chiueh, David Eichler, Michael Gedalin, Edward Liverts, Yury Lyubarsky, Irena Shuster, Raphael Steinitz, and Chi Yuan for several valuable discussions and constructive criticism of the manuscript. Part of this work has been conducted under the auspices of the Israeli Ministry of Immigrant Absorption program "KAMEA." Support was also received from the Israel Science Foundation and the Binational U.S.–Israel Science Foundation.

References

- Bertin, & Casertano, S. 1982, *Astron. Astrophys.* 106, 274
- Bridges, F.G., Hatzes, A.P. & Lin, D.N.C. 1984, *Nature* 309, 333
- Cuzzi, J.N., Colwell, J.E., Esposito, L.W., *et al.* 2002, *Space Sci. Rev.* 118, 209
- Daisaka, H. & Ida, S. 1999, *Earth Planets Space* 51, 1195
- Esposito, L.W. 1993, *ARE&PS* 21, 487
- Esposito, L.W. 2002, *Rep. Prog. Phys.* 65, 1741
- Goldreich, P. & Tremaine, S. 1982, *ARA&A* 20, 249
- Griv, E. 1996, *Planet. Space Sci.* 44, 579
- Griv, E. 1998, *Planet. Space Sci.* 46, 615
- Griv, E. & Gedalin, M. 2003, *Planet. Space Sci.* 51, 899
- Griv, E., Gedalin, M., Eichler, D. & Yuan, C. 2000, *Planet. Space Sci.* 48, 679
- Griv, E., Rosenstein, B., Gedalin, M. & Eichler, D. 1999, *Astron. Astrophys.* 347, 821
- Griv, E., Gedalin, M. & Yuan, C. 2003a, *Astron. Astrophys.*, 400, 375
- Griv, E., Gedalin, M. & Yuan, C. 2003b, *Mon. Not. R. Astron. Soc.* 342, 1102
- Kerr, R.A. 1985, *Science* 220, 1376
- Lane, A.L., Hord, C.W., West, R.A., *et al.* 1982, *Science* 215, 537
- Lin, C.C. & Shu F.H. 1966, *Proc. Natl. Acad. Sci.* 55, 229
- Lin, C.C. & Lau, Y.Y. 1979, *SIAM Stud. Appl. Math.* 60, 97
- Lin, C.C., Yuan, C. & Shu, F.H. 1969, *Astrophys. J.* 155, 721
- Lissauer, J.J. & Cuzzi, J.N. 1985, in: D.C. Black & M.S. Matthews (Eds.), *Protostars and Planets, II*, Univ. of Arizona Press, p. 920
- Ohtsuki, K. & Emori, H. 2000, *Astrophys. J.* 119, 403
- Osterbart, R. & Willerding, E. 1995, *Planet. Space Sci.* 43, 289
- Richardson, D.C. 1994, *Mon. Not. R. Astron. Soc.* 269, 493
- Safronov, V.S. 1960, *Ann. d'Astrophys.* 23, 979
- Salo, H. 1992, *Nature* 359, 619
- Salo, H. 1995, *Icarus* 117, 287
- Shu, F.H. 1970, *Astrophys. J.* 160, 99
- Smith, B.A., Soderblom, L., Batson, R., *et al.* 1982, *Science* 215, 504
- Sterzik, M.F., Herold, H., Ruder, H. & Willerding, E. 1995, *Planet. Space Sci.* 43, 259
- Toomre, A. 1964, *Astrophys. J.* 139, 1217
- Toomre, A. 1990, in: R. Wielen (Ed.), *Dynamics and Interactions of Galaxies*, Springer-Verlag, p. 292
- Toomre, A. & Kalnajs, A.J. 1991, in: B. Sundelius (Ed.), *Dynamics of Disc Galaxies*, Göteborg Univ. Press, p. 341
- Tremaine, S. 2003, *Astron. J.* 125, 894
- Wisdom, J. & Tremaine, S. 1988, *Astron. J.* 95, 925
- Zebker, H.A., Marouf, E.A. & Tyler, G.L. 1985, *Icarus* 64, 531